Vol. 29 (1998) ACTA PHYSICA POLONICA B No 12

THE KONDO LATTICE MODEL*

M. Lavagna†

Commissariat à l'Energie Atomique, DRFMC /SPSMS, 17, rue des Martyrs
38054 Grenoble Cedex 9, France

and C. Pépin

University of Oxford, Department of Physics
1 Kable Road, OX1 3NP Oxford, UK

(Received November 26, 1998)

In this lecture, we review the experimental situation of heavy fermions with emphasis on the existence of a quantum phase transition (QPT) and related non-Fermi liquid (NFL) effects. We overview the Kondo-Lattice Model (KLM) which is believed to describe the physics of those systems. After recalling the existing theories based on large-N expansion and various N=2 schemes, we present two alternative approaches: *(i)* a spin fluctuation Kondo functional integral approach treating the spin-fluctuation and Kondo effects on an equal footing, and *(ii)* a supersymmetric theory enlarging the usual fermionic representation of the spin into a mixed fermionic-bosonic representation in order to describe the spin degrees of freedom as well as the Fermi-liquid type excitations. This kind of approaches may open up new prospects for the description of the critical phenomena associated with the quantum phase transition in heavy-fermion systems.

PACS numbers: 75.30.Mb, 71.27.+a

1. Experimental overview

In heavy-fermion systems with $4f$ or $5f$ atoms (such as Ce or U), the proximity of the electronic orbital to the Fermi level confers a Kondo effect at low temperature, *i.e.* an on-site compensation of localized magnetic moment by conduction electrons [1]. A direct consequence is the observation at low temperature of a very large effective electronic mass m^* derived from the huge linear specific heat coefficient $\gamma = C/T$ and a correspondingly

* Presented at the XXXVIII Cracow School of Theoretical Physics, Zakopane, Poland, June 1–10, 1998.

† Also at the Centre National de la Recherche Scientifique (CNRS).

large Pauli susceptibility. Simultaneously, the realization of the de Haas–van Alphen (dH–vA) quantum oscillations [2] also concludes in favour of the existence of heavy quasiparticles.

In addition to the Kondo effect, those systems are characterized by long-range RKKY (Ruderman–Kittel–Kasuya–Yoshida) interactions between neighboring local moments mediated by conduction electrons. The competition between the Kondo effect and the RKKY interactions leads to the possibility of either a non-magnetic or a long-range magnetically-ordered ground state [3]. A zero-temperature quantum phase transition occurs governed by the value of the exchange coupling J between the spin of the conduction electron and the local moment. One of the most striking properties of the heavy-fermion compounds discovered these last years is the experimental possiblity to explore this quantum phase transition [4–7] by varying the composition change (as in Ce $Cu_{6-x}Au_x$ or $Ce_xLa_{1-x}Ru_2Si_2$), or by applying a pressure or a magnetic field. Thus a magnetic instability is observed at $x_c = 0.1$ in $CeCu_{6-x}Au_x$ [4], and $x_c = 0.08$ in $Ce_xLa_{1-x}Ru_2Si_2$ [7]. For $x = x_c$, where $T_{\rm N} = 0$, the observed behavior at low temperature is at odds with that usually expected for a simple Fermi liquid (FL). In Ce $Cu_{6-x}Au_x$, the specific heat C depends on T as $C/T \sim -\ln(T/T_0)$, the magnetic susceptibility as $\chi \sim 1 - \alpha\sqrt{T}$, and the T-dependent part of the resistivity as $\Delta\rho \sim T$ (instead of $C/T \sim \chi \sim$ const and $\Delta\rho \sim T^2$ in the Fermi liquid state). Pressure or large magnetic fields are found to restore the FL behavior.

The origin of this non-Fermi liquid (NFL) regime is a largely discussed problem. The three main interpretations which have been proposed rely on (*i*) a single impurity multichannel Kondo effect in which the internal degree of freedom is provided by the $4f$ or $5f$ quadrupolar moment [8], (*ii*) a distribution of the Kondo coupling due to the disorder leading to a distribution of the Kondo temperature $P(T_{\rm K})$ [9] and (*iii*) the proximity of a quantum phase transition [10–15] as is emphasized in this course.

Another important insight is provided by the Inelastic Neutron Scattering (INS) experiments carried out in systems close to the magnetic instability. The measurements performed in pure compounds $CeCu_6$ or $CeRu_2Si_2$ [16, 17] have shown the presence of two distinct contributions to the dynamic magnetic structure factor: a q-independent quasielastic component, and a strongly q-dependent inelastic contribution peaked at the value $\omega_{\rm max}$ of the frequency. The same experiments carried out in systems with varying concentrations as $Ce_xLa_{1-x}Ru_2Si_2$ [18] , show a shift of $\omega_{\rm max}$ to zero when getting near the magnetic instability. Any theory aimed to describe the quantum critical phenomena in heavy-fermion compounds should account for the so-quoted behavior of the dynamical spin susceptibility.

2. Theoretical overview

The model which is believed to describe the heavy-fermion systems is the Periodic Anderson Model (PAM) defined for the case of spin 1/2 [19] as

$$H = \sum_{k\sigma} \varepsilon_k c^\dagger_{k\sigma} c_{k\sigma} + E_0 \sum_{i\sigma} f^\dagger_{i\sigma} f_{i\sigma} + V \sum_{i\sigma} (c^\dagger_{i\sigma} f_{i\sigma} + \text{c.c.}) + U \sum_i n^\uparrow_{fi} n^\downarrow_{fi} \,, \quad (1)$$

where $n^\sigma_{fi} = f^+_{i\sigma} f_{i\sigma}$. It describes the conduction electrons $c_{k\sigma}$ with dispersion ε_k which hybridize with the localized f electrons of energy E_0. The grand canonical ensemble is used and both energies ε_k and E_0 are measured from the chemical potential μ. The hybridization matrix element is approximated by a constant V. U represents the on-site Coulomb repulsion between f electrons.

In the Kondo limit, a canonical transformation allows to change the Periodic Anderson Model into the Kondo-Lattice Model (KLM) defined as

$$H = \sum_{k\sigma} \varepsilon_k c^\dagger_{k\sigma} c_{k\sigma} + J \sum_i \boldsymbol{s}_i . \boldsymbol{S}_i \,, \quad (2)$$

where J is the on-site Kondo coupling between the spin of the conduction electrons $\boldsymbol{s}_i = \sum_{\sigma\sigma'} c^\dagger_{i\sigma} \boldsymbol{\tau}_{\sigma\sigma'} c_{i\sigma'}$ and the localized spin represented by $\boldsymbol{S}_i = \sum_{\sigma\sigma'} f^\dagger_{i\sigma} \boldsymbol{\tau}_{\sigma\sigma'} f_{i\sigma'}$ in the Abrikosov pseudo-fermionic representation of the spin imposing the constraint $n_{fi} = \sum_\sigma n^\sigma_{fi} = 1$. That canonical transformation analogous to the Schrieffer–Wolf transformation for the single-impurity case is valid in the regime $|\varepsilon_k| \ll (-E_0)$ and $|\varepsilon_k| \ll |E_0 + U|$. One gets: $J = V^2 \left[-\frac{1}{E_0} + \frac{1}{E_0 + U} \right]$. In the $U \to \infty$ limit, one has $J = -V^2/E_0$ while in the symmetric Anderson model defined by $E_0 = -U/2$, the result is $J = 4V^2/U$. The Kondo-lattice model has been first introduced by Doniach in 1977 [3] and we refer to the paper of Tsunetsugu *et al.* [20] for an extensive review on the KLM essentially at D=1.

Let us first recall the main physical ideas behind the Kondo-lattice model: (*i*) the competition between the Kondo effect and the RKKY interactions leading to the so-called "Doniach phase diagram" and (*ii*) the nature of the screening of the local moments in the lattice.

Concerning the point (*i*), the competition between the Kondo effect on each site which tends to suppress the magnetic moment with decreasing temperature and the RKKY interactions which, on the contrary, tend to magnetically order the local moments, leads to the well-known Doniach phase diagram [3]. Let us call $T^0_{\rm K}$ the Kondo temperature for the single-impurity and $T^0_{\rm N}$ (or $T^0_{\rm C}$) the Néel (or Curie) temperatures in the absence of Kondo effect: $T^0_{\rm K} = D \exp(-1/\rho_0 J)$ and $T^0_{\rm N} \sim (\rho_0 J)^2$, where D and ρ_0 are the bandwidth and the density of states at the Fermi level of the conduction electron band. Thus, at small $\rho_0 J$, $T_{\rm N}^0$ is larger than $T_{\rm K}^0$ and a long-range magnetic order is established with, eventually, a reduction of the magnetic moment due to the Kondo effect. Oppositely, at large $\rho_0 J$, $T_{\rm K}^0$ is larger than $T_{\rm N}^0$, the Kondo effect wins and the system does not order magnetically. Therefore, the real Néel temperature $T_{\rm N}$ first increases with increasing $\rho_0 J$, passes through a maximum and finally goes to zero at a critical value of the coupling $\rho_0 J_C$ giving rise to a zero-temperature quantum critical point.

As far as the nature of the screening is concerned (point (*ii*)), an important idea advanced by Nozières [21] is the possibility of an exhaustion of the conduction electrons in the screening of the local moments. In the single-impurity Kondo case, at low temperature, the local moment is screened by the conduction electrons and a spin-singlet state is formed. In this so-called Kondo effect, the number of conduction electrons in the screening cloud formed around the impurity is equal to 1. In the Kondo lattice case, the number of conduction electrons which are available are to be taken within a thermal window of width $k_{\rm B}T$ around the Fermi level. It should be compared to the number of sites $N_{\rm S}$ to be screened. Depending on the value of the parameters, some situations may occur where the available conduction electrons are "exhausted" before achieving complete screening leaving residual unscreened spin degrees of freedom on the impurities. That idea of "uncomplete" Kondo effect is at the root of the supersymmetric theory that we propose later on.

At high temperature, pertubation techniques in J may be applied leading to the famous Kondo minimum in the resistivity as a function of temperature. Those pertubation techniques fail below the Kondo temperature and there is a need for other techniques to solve the problem at low-temperature. The other approaches based on the Bethe ansatz and the Renormalizaion Group which revealed very powerful in the single-impurity case cannot be generalized to the lattice case. In that context, there has been an intensive search for new approaches among which the large-N and more generally the functional integral approaches described here.

2.1. The large-N expansion

An important breakthrough in the understanding of the periodic Anderson Model occured about 15 years ago when the idea of slave-bosons was introduced: [22, 23] for the single-impurity case, [24–27] for the lattice. In the limit of large on-site Coulomb repulsion ($U \to \infty$), where the double-occupancy is energetically forbidden, one can introduce a slave-boson representation in which the two allowed states *i.e.* the empty or the singly-occupied states are represented by $e_i^\dagger|0\rangle$ and $f_{i\sigma}^\dagger|0\rangle$. The exclusion of double-occupancy is expressed as

$$P_i = e_i^\dagger e_i + \sum_\sigma f_{i\sigma}^\dagger f_{i\sigma} - 1 = 0\,. \qquad (3)$$

The physical electron creation operator which creates transitions between empty and singly-occupied sites is represented by $f_{i\sigma}^\dagger e_i$, while the number of f electrons on site i of spin σ is equal to $f_{i\sigma}^\dagger e_i e_i^\dagger f_{i\sigma} = f_{i\sigma}^\dagger f_{i\sigma}$ provided that the local constraint is satisfied. Hence the slave-boson representation of the $U \to \infty$ PAM Hamiltonian is given by

$$H = \sum_{k,\sigma} \varepsilon_k c_{k\sigma}^\dagger c_{k\sigma} + E_0 \sum_{i,\sigma} f_{i\sigma}^\dagger f_{i\sigma} + V \sum_{i,\sigma} (c_{i\sigma}^\dagger e_i^\dagger f_{i\sigma} + \text{c.c.}) \qquad (4)$$

provided that the local constraint Eq. (3) is satisfied that is enforced with the aid of a time-independent Lagrange multiplier λ_i. The operators e_i^+ and $f_{i\sigma}^+$ obey bosonic and fermionic statistics, respectively.

It is then convenient to generalize the original PAM model from SU(2) to SU(N) by allowing for the spin index σ in Eq. (4) to run from $-S$ to S. That corresponds to the situation of impurities of spin S coupled to conduction electrons of degeneracy N with $N = 2S + 1$. The corresponding SU(N) model is interesting because it can be solved exactly in the limit $N \to \infty$. For this limit to make sense, the hybridization matrix element V should be scaled as $1/\sqrt{N}$ therefore $V = \widetilde{V}/\sqrt{N}$.

We do not give here all the details of the calculations which can be found in the litterature. Let us say that the saddle-point approximation which consists of taking e_i and λ_i as site-independent (as well as time-independent for e_i) is exact in the limit $N \to \infty$. It leads to the formation of two quasiparticle bands of energies $E_k^\pm = \frac{1}{2}\varepsilon_k + \varepsilon_f \pm \sqrt{(\varepsilon_k - \varepsilon_f)^2 + 4V^2 e_0^2}$, where $\varepsilon_f = E_0 + \lambda_0$. The values of e_0, ε_f and μ are fixed by the saddle-point equations. The two bands are split by a hybridization gap and the density of states at the Fermi level is strongly renormalized $\rho(E_\text{F}) \sim 1/T_\text{K}$, where $T_\text{K} = D\exp(E_0/\rho_0 V^2)$. The specific heat coefficient γ and the magnetic susceptibility χ are also strongly enhanced with the Wilson ratio χ/γ equal to 1. Oppositely, the charge susceptibility is found to be unenhanced. The ground state corresponds to a collective Kondo screening in which only a fraction of conduction electons equal to T_K/D screens each of the impurities.

Next step is to include the gaussian fluctuations around the saddle-point. The corresponding corrections in $1/N$ generate effective interactions among the quasiparticles which can be analyzed in terms of Landau paramaters. In the case of the multichannel single-Kondo impurity problem, conserving T-matrix approximation methods [28] have been extensively used to derive the finite temperature behavior with very accurate comparison with the Bethe ansatz and Conformal Field theory results. The generalization to the case of the lattice has still to be done. All the results can be reproduced by starting instead from the $N \to \infty$ Kondo lattice Hamiltonian and performing a Hubbard–Stratonovich transformation on the coupling term making the field Φ appear. There is then a one-to-one equivalence between $\Phi_0 = J \sum_{k\sigma} \langle c^\dagger_{k\sigma} f_{k\sigma} \rangle$ and Ve_0. In all cases, no magnetic instability is found at the order $1/N$ since the RKKY interactions occur at the order $1/N^2$ [29]. The latter point constitutes a serious drawback of the large-N expansion which makes it inappropriate to describe the Quantum Critical Point observed experimentally. The fact that the slave-boson does not carry spin implies that spin and charge fluctuations cannot be treated on an equal footing contrary to what happens with other slave-boson representations as the one introduced by Kotliar and Ruckenstein that we present now.

2.2. The different N=2 approaches

In the case of a degeneracy $N = 2$ ($S = 1/2$), Kotliar and Ruckenstein (KR) [30] introduced 4 slave-bosons e_i, $p_{i\sigma}$ and d_i in order to keep track of the 4 possible local configurations so that the empty $|O\rangle_i$, the singly-occupied $|\sigma\rangle_i$ and the doubly-occupied $|\uparrow\downarrow\rangle_i$ states are represented by: $|O\rangle_i = e^\dagger_i |\text{vac}\rangle$, $|\sigma\rangle_i = p^\dagger_{i\sigma} f^\dagger_{i\sigma} |\text{vac}\rangle$ and $|\uparrow\downarrow\rangle_i = d^\dagger_i f^\dagger_{i\uparrow} f^\dagger_{i\downarrow} |\text{vac}\rangle$, where e_i, $p_{i\sigma}$ and d_i are bosons and $f_{i\sigma}$ fermions. Then the PAM can be written as

$$H = \sum_{k,\sigma} \varepsilon_k c^\dagger_{k\sigma} c_{k\sigma} + E_0 \sum_{i,\sigma} f^\dagger_{i\sigma} f_{i\sigma} + V \sum_{i,\sigma} (c^\dagger_{i\sigma} f_{i\sigma} z_{i\sigma} + \text{c.c.}) + U \sum_i d^\dagger_i d_i \quad (5)$$

with

$$z_{i\sigma} = \left(e^\dagger_i p_{i\sigma} + p^\dagger_{i-\sigma} d_i \right) / \left[\sqrt{1 - e^\dagger_i e_i - p^\dagger_{i-\sigma} p_{i-\sigma}} \sqrt{1 - d^\dagger_i d_i - p^\dagger_{i\sigma} p_{i\sigma}} \right]$$

provided that the 3 following constraints are fulfilled

$$\begin{aligned} P_i &= e^\dagger_i e_i + \sum_\sigma p^\dagger_{i\sigma} p_{i\sigma} - 1 = 0\,, \\ Q_{i\sigma} &= f^\dagger_{i\sigma} f_{i\sigma} - (p^\dagger_{i\sigma} p_{i\sigma} + d^\dagger_i d_i) = 0\,. \end{aligned} \quad (6)$$

The choice of the denominator in $z_{i\sigma}$ guarantees to recover the free electron gaz limit at $U \to 0$. This representation first introduced in the case of the Hubbard model was shown at the saddle-point level to give back the variational Gutzwiller approximation (GA) as developed by Rice and Ueda [31]. It then allows to include the gaussian fluctuations around the GA solution [32, 33]. In the case of the PAM [34, 36, 39, 40], the KR representation already leads to interesting results at the saddle-point level as soon as staggered symmetry-broken state appropriate for bipartite lattice with nesting is allowed. Notably, at d=1 [34], the approach essentially gives the same results as those obtained by the variational wave function approach of Gulacsi, Strack and Vollhardt [35]. At infinite dimension [36], a phase transition to the antiferromagnetic insulator is found below a critical value $V_{\rm C}$ of the hybridization matrix element consistent with the Doniach predictions and in quantitative agreement with the $d = \infty$ QMC [37] and exact diagonalization [38] results. The general phase diagram for the three-dimensional case has been determined by Doradzinski and Spalek [39]. Those studies enlighten on the nature of the moment compensation which takes place in the antiferromagnetic state. The study of the V-dependence of the staggered magnetizations m_f and m_c shows an almost total moment compensation of m_f and m_c near $V_{\rm C}$ suggesting an itinerant magnetism in which f and c electrons are part of the same quasiparticles. Oppositely, in the $V \to 0$ limit, m_f saturates while m_c goes to zero indicating a local moment magnetism. Figure 4 of paper [39] illustrates the latter point by showing the V-dependence of m_f and m_c in the antiferromagnetic insulating state.

Finally, other path integral approaches to the KLM have been proposed based on different Hubbard–Stratonovich decouplings of the exchange term [41, 42]. For the extended KLM in which the Heisenberg interactions among neighboring sites are included, we will mention the work of Coleman and Andrei [42] which consists in keeping the Resonant Valence Bond (RVB) parameter $\chi_{ij} = J \sum_\sigma f^\dagger_{i\sigma} f_{j\sigma}$ on neighboring sites at the same time as the Kondo parameter $\Phi = J \sum_\sigma c^\dagger_{i\sigma} f_{i\sigma}$ quoted before. This approach leads to the stabilization of a spin-liquid state at low temperature with possible anisotropic superconducting instability. This approach has been used in a recent paper by Iglesias, Lacroix and Coqblin [43] where they propose a revisited version of the Doniach phase diagram in which the Kondo temperature is drastically reduced resulting of the formation of the resonant valence bonds.

In the rest of the paper, we will develop two alternative approaches to the Kondo-lattice model: (i) the first one consists in keeping the f and c magnetizations at the same level as the Kondo parameter [15]. We will show how it is possible to account for the spin-fluctuation and the Kondo effects on an equal footing thus combining both large N and spin-fluctuation theories. To our point of view, this approach constitutes an ideal framework to study the quantum critical phenomena around the magnetic transition; (ii) the second approach consists in enlarging the usual Abrikosov pseudo-fermionic representation of the spin into a mixed fermionic-bosonic representation in order to describe the spin degrees of freedom as well as the Fermi-liquid type excitations [44]. The analogy of the approach with the supersymmetry theory of disordered systems leads to giving it the nickname of "supersymmetric approach".

3. The spin fluctuation-Kondo functional integral approach

In the grand canonical ensemble, the Hamiltonian of the Kondo-Lattice Model (KLM) constituted by a periodic array of Kondo impurities with an average number of conduction electrons per site n_c is written as

$$H=\sum_{k\sigma}\varepsilon_k c^\dagger_{k\sigma}c_{k\sigma}+J\sum_i \boldsymbol{S}_i\cdot\sum_{\sigma\sigma'}c^\dagger_{i\sigma}\boldsymbol{\tau}_{\sigma\sigma'}c_{i\sigma'}-\mu N_S\left(\frac{1}{N_{\rm S}}\sum_{k\sigma}c^\dagger_{k\sigma}c_{k\sigma}-n_c\right) \quad (7)$$

in which $\boldsymbol{\tau}$ are the Pauli matrices $(\boldsymbol{\tau}^x,\boldsymbol{\tau}^y,\boldsymbol{\tau}^z)$ and $\boldsymbol{\tau}^0$ the unit matrix; J is the antiferromagnetic Kondo interaction $(J>0)$.

We use the Abrikosov pseudofermion representation of the spin $\boldsymbol{S}_i$: $\boldsymbol{S}_i=\sum_{\sigma\sigma'} f^\dagger_{i\sigma}\boldsymbol{\tau}_{\sigma\sigma'}f_{i\sigma'}$. The projection into the physical subspace is implemented by a local constraint

$$Q_i=\sum_\sigma f^+_{i\sigma}f_{i\sigma}-1=0\,. \quad (8)$$

A Lagrange multiplier λ_i is introduced to enforce the local constraint Q_i. Since $[Q_i,H]=0$, λ_i is time-independent.

In this representation, the partition function of the KLM can be expressed as a functional integral over the coherent states of the Fermion fields

$$Z=\int \mathcal{D}c_{i\sigma}\mathcal{D}f_{i\sigma}d\lambda_i\exp\left[-\int_0^\beta \mathcal{L}(\tau)d\tau\right]\,, \quad (9)$$

where the Lagrangian $\mathcal{L}(\tau)$ is given by

$$\begin{aligned}\mathcal{L}(\tau) &= \mathcal{L}_0(\tau)+H_0(\tau)+H_J(\tau)\,,\\ \mathcal{L}_0(\tau) &= \sum_{i\sigma}c^\dagger_{i\sigma}\partial_\tau c_{i\sigma}+f^\dagger_{i\sigma}\partial_\tau f_{i\sigma}\,,\end{aligned}$$

$$\begin{aligned}H_0(\tau) &= \sum_{k\sigma}\varepsilon_k c^\dagger_{k\sigma}c_{k\sigma}-\mu N_{\rm S}\left(\frac{1}{N_{\rm S}}\sum_{k\sigma}c^\dagger_{k\sigma}c_{k\sigma}-n_c\right)+\sum_i\lambda_i Q_i\,,\\ H_J(\tau) &= J\sum_i \boldsymbol{S}_{fi}\cdot\boldsymbol{S}_{ci}\end{aligned}$$

with $\quad \boldsymbol{S}_{c_i}=\sum_{\sigma\sigma'}c^\dagger_{i\sigma}\boldsymbol{\tau}_{\sigma\sigma'}c_{i\sigma'} \quad$ and $\quad \boldsymbol{S}_{fi}=\boldsymbol{S}_i\,.$

We perform a Hubbard–Stratonovich transformation on the Kondo interaction term $H_J(\tau)$. Since more than one field is implied in the transformation, an uncertainty is left on the way of decoupling. We propose to remove it in the following way. First, we note that $H_J(\tau)$ may also be written as

$$H_J(\tau) = -\frac{3J}{8}\sum_i n_{fc_i}n_{cf_i} + \frac{J}{2}\sum_i \boldsymbol{S}_{fc_i}\cdot\boldsymbol{S}_{cf_i}\,, \tag{10}$$

where $\boldsymbol{S}_{fc_i} = \sum\limits_{\sigma\sigma'} f^\dagger_{i\sigma}\boldsymbol{\tau}_{\sigma\sigma'}c_{i\sigma'}$ and $n_{fc_i} = \sum\limits_{\sigma\sigma'} f^\dagger_{i\sigma}\tau^0_{\sigma\sigma'}c_{i\sigma'}$ (respectively $\boldsymbol{S}_{cf_i}$ and n_{cf_i} their Hermitian conjugate).

The Kondo interaction term is then given by any linear combination of $J\sum\limits_i \boldsymbol{S}_{fi}\cdot\boldsymbol{S}_{ci}$ (with a weighting factor x) and of the term appearing in the right-hand side of equation (10) (with a weighting factor (1-x)). x is chosen so as to recover the usual results obtained within the slave-boson theories [24–27]. One can check that this is the case for $x = 1/3$. The Kondo interaction term is then given by

$$H_J(\tau) = J_S\sum_i(\boldsymbol{S}_{f_i}\cdot\boldsymbol{S}_{c_i} + \boldsymbol{S}_{fc_i}\cdot\boldsymbol{S}_{cf_i}) - J_C\sum_i n_{fc_i}n_{cf_i} \tag{11}$$

with $J_S = J/4$ and $J_C = J/3$.

Performing a generalized Hubbard–Stratonovich transformation on the partition function Z makes the fields Φ_i, Φ^*_i (for charge) and $\boldsymbol{\xi}_{f_i}$, $\boldsymbol{\xi}_{c_i}$ appear (omitting the fields associated to $\boldsymbol{S}_{fc_i}$, $\boldsymbol{S}_{cf_i}$). We get

$$Z = \int d\Phi_i d\Phi^*_i d\boldsymbol{\xi}_{f_i} d\boldsymbol{\xi}_{c_i}\mathcal{D}c_{i\sigma}\mathcal{D}f_{i\sigma}d\lambda_i \exp\left[-\int_0^\beta \mathcal{L}'(\tau)d\tau\right] \tag{12}$$

with

$$\mathcal{L}'(\tau) = \mathcal{L}_0(\tau) + H_0(\tau) + H'_J(\tau)\,,$$

$$\begin{aligned} H'_J(\tau) \;=\; & \sum_{i\sigma\sigma'}\left(c^\dagger_{i\sigma}, f^\dagger_{i\sigma}\right)\begin{pmatrix} -J_S i\boldsymbol{\xi}_{f_i}\cdot\boldsymbol{\tau}_{\sigma\sigma'} & J_C\Phi^*_i\tau^0_{\sigma\sigma'} \\ J_C\Phi_i\tau^0_{\sigma\sigma'} & -J_S i\boldsymbol{\xi}_{c_i}\cdot\boldsymbol{\tau}_{\sigma\sigma'}\end{pmatrix}\begin{pmatrix} c_{i\sigma'} \\ f_{i\sigma'}\end{pmatrix} \\ & + J_C\sum_i \Phi^*_i\Phi_i + J_S\sum_i \boldsymbol{\xi}_{f_i}.\boldsymbol{\xi}_{c_i}\,. \end{aligned}$$

3.1. Saddle point

The saddle-point solution is obtained for space and time independent fields Φ_0, λ_0, ξ_{f_0} and ξ_{c_0}. In the magnetically-disordered regime ($\xi_{f_0} = \xi_{c_0} = 0$), it leads to renormalized bands α and β as schematized in figure 1. Noting $\sigma_0^{(*)} = J_C \Phi_0^{(*)}$ and $\varepsilon_f = \lambda_0$, $\alpha^\dagger_{k\sigma}|0\rangle$ and $\beta^\dagger_{k\sigma}|0\rangle$ are the eigenstates of

$$\boldsymbol{G}_0^{-1\sigma}(\boldsymbol{k},\tau) = \begin{pmatrix} \partial_\tau + \varepsilon_k & \sigma_0^* \\ \sigma_0 & \partial_\tau + \varepsilon_f \end{pmatrix} \tag{13}$$

with respectively the eigenenergies $(\partial_\tau + E_k^-)$ and $(\partial_\tau + E_k^+)$. In the notations: $x_k = \varepsilon_k - \varepsilon_f$, $y_k^\pm = E_k^\pm - \varepsilon_f$ and $\Delta_k = \sqrt{x_k^2 + 4\sigma_0^2}$, we get

$$y_k^\pm = (x_k \pm \Delta_k)/2\,. \tag{14}$$

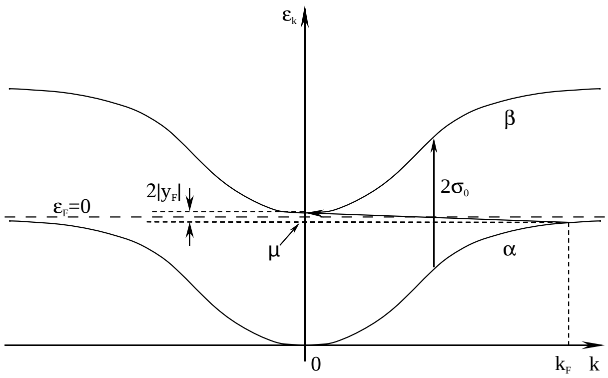

Fig. 1. Energy versus wave-vector k for the two bands α and β. Note the presence of a direct gap of value $2\sigma_0$ and of an indirect gap of value $2\,|y_{\rm F}|$.

Let us note $U^\dagger_{k\sigma}$ the matrix transforming the initial basis ($c^\dagger_{k\sigma}$, $f^\dagger_{k\sigma}$) to the eigenbasis ($\alpha^\dagger_{k\sigma}$, $\beta^\dagger_{k\sigma}$). The Hamiltonian being Hermitian, the matrix $U_{k\sigma}$ is unitary : $U_{k\sigma}U^\dagger_{k\sigma} = U^\dagger_{k\sigma}U_{k\sigma} = 1$. In the notation $U^\dagger_{k\sigma} = \begin{pmatrix} -v_k & u_k \\ u_k & v_k \end{pmatrix}$, we have

$$\begin{aligned} u_k &= \frac{-\sigma_0/y_k^-}{\sqrt{1+(\sigma_0/y_k^-)^2}} = \frac{1}{2}\left[1 + \frac{x_k}{\Delta_k}\right], \\ v_k &= \frac{1}{\sqrt{1+(\sigma_0/y_k^-)^2}} = \frac{1}{2}\left[1 - \frac{x_k}{\Delta_k}\right]. \end{aligned} \tag{15}$$

The saddle-point equations together with the conservation of the number of conduction electrons are written as

$$\begin{aligned}
\sigma_0 &= \frac{1}{N_{\rm S}} J_C \sum_{k\sigma} u_k v_k \; n_{\rm F}(E_k^-) \,, \\
1 &= \frac{1}{N_{\rm S}} \sum_{k\sigma} u_k^2 \; n_{\rm F}(E_k^-) \,, \\
n_c &= \frac{1}{N_{\rm S}} \sum_{k\sigma} v_k^2 \; n_{\rm F}(E_k^-) \,. \qquad (16)
\end{aligned}$$

Their resolution leads to

$$\begin{aligned}
&|y_{\rm F}| = D \exp\left[-2/\left(\rho_0 J_C\right)\right] \,, \\
&2\rho_0 \sigma_0^2 / \left|y_{\rm F}\right| = 1 \,, \\
&\mu = 0 \,, \qquad (17)
\end{aligned}$$

where $y_{\rm F} = \mu - \varepsilon_{\rm F}$ and ρ_0 is the bare density of states of conduction electrons ($\rho_0 = 1/2D$ for a flat band). Noting $y = E - \varepsilon_{\rm F}$, the density of states at the energy E is $\rho\,(E) = \rho_0 \left(1 + \sigma_0^2/y^2\right)$. If $n_c < 1$, the chemical potential is located just below the upper edge of the α band. The system is metallic. The density of states at the Fermi level is strongly enhanced towards the bare density of states of conduction electrons: $\rho(E_{\rm F})/\rho_0 = (1 + \sigma_0^2/y_{\rm F}^2) \sim 1/(2\rho_0 \left|y_{\rm F}\right|)$. That corresponds to the flat part of the α band in figure 1. It is associated to the formation of a Kondo or Abrikosov–Suhl resonance pinned at the Fermi level resulting of the Kondo effect. The low-lying excitations are quasiparticles of large effective mass m^* as observed in heavy-fermion systems. Also note the presence of a hybridization gap between the α and the β bands. The direct gap of value $2\sigma_0$ is much larger than the indirect gap equal to $2|y_{\rm F}|$. The saddle-point solution transposes to $N{=}2$ the large-N results obtained within the slave-boson mean-field theories [24–27].

3.2. Gaussian fluctuations

We now consider the gaussian fluctuations around the saddle-point solution. Following Read and Newns [23], we take advantage of the local U(1) gauge transformation of the Lagrangian $\mathcal{L}'(\tau)$

$$\begin{aligned}
\varPhi_i &\rightarrow r_i \exp(i\theta_i) \,, \\
f_i &\rightarrow f_i' \exp(i\theta_i) \,, \\
\lambda_i &\rightarrow \lambda_i' + i \; \partial\theta_i/\partial\tau \,.
\end{aligned}$$

We use the radial gauge in which the modulus of both fields $\varPhi_i$ and $\varPhi_i^*$ are the radial field r_i, and their phase θ_i (via its time derivative) is incorporated into the Lagrange multiplier λ_i which turns out to be a field. Use of the radial instead of the Cartesian gauge bypasses the familiar complications of infrared divergences associated with unphysical Goldstone bosons. We let the fields fluctuate away from their saddle-point values : $r_i = r_0 + \delta r_i$, $\lambda_i = \lambda_0 + \delta\lambda_i$, $\boldsymbol{\xi}_{f_i} = \delta\boldsymbol{\xi}_{f_i}$ and $\boldsymbol{\xi}_{c_i} = \delta\boldsymbol{\xi}_{c_i}$. After integrating out the Grassmann variables in the partition function in equation (12), we get

$$Z = \int \mathcal{D}r_i \mathcal{D}\lambda_i \mathcal{D}\boldsymbol{\xi}_{f_i} \mathcal{D}\boldsymbol{\xi}_{c_i} \exp\left[-S_{\text{eff}}\right], \tag{18}$$

where the effective action is

$$S_{\text{eff}} = -\sum_{k,i\omega_n} \ln \text{Det}\boldsymbol{G}^{-1}(\boldsymbol{k}, i\omega_n) + \beta\,[\, J_C \sum_i r_i^2 + J_S \sum_i \boldsymbol{\xi}_{f_i}\cdot\boldsymbol{\xi}_{c_i} + N_{\text{S}}(\mu n_c - \lambda_0)]$$

with :

$$\left[\boldsymbol{G}^{-1}(i\omega_n)\right]_{ij}^{\sigma\sigma'} = \begin{pmatrix} A_{11} & A_{12} \\ A_{21} & A_{22} \end{pmatrix},$$

where

$$\begin{aligned}
A_{11} &= [(-i\omega_n - \mu)\delta_{ij} - t_{ij}]\delta_{\sigma\sigma'} - J_S i\boldsymbol{\xi}_{f_i}.\boldsymbol{\tau}_{\sigma\sigma'}\delta_{ij}\,, \\
A_{12} &= A_{21} = (\sigma_0 + J_C\delta r_i)\delta_{\sigma\sigma'}\delta_{ij}\,, \\
A_{22} &= [-i\omega_n + \varepsilon_f + \delta\lambda_i]\delta_{\sigma\sigma'}\delta_{ij} - J_S i\boldsymbol{\xi}_{c_i}.\boldsymbol{\tau}_{\sigma\sigma'}\delta_{ij}\,.
\end{aligned}$$

Expanding up to the second order in the Bose fields, one obtains the Gaussian corrections $S_{\text{eff}}^{(2)}$ to the saddle-point effective action

$$\begin{aligned}
S_{\text{eff}}^{(2)} = \frac{1}{\beta}\sum_{\boldsymbol{q},i\omega_\nu} \Bigg[& \begin{pmatrix} \delta r, & \delta\lambda \end{pmatrix} \boldsymbol{D}_C^{-1}(\boldsymbol{q}, i\omega_\nu) \begin{pmatrix} \delta r \\ \delta\lambda \end{pmatrix} \\
& + \begin{pmatrix} \delta\xi_f^z, & \delta\xi_c^z \end{pmatrix} \boldsymbol{D}_S^{\parallel -1}(\boldsymbol{q}, i\omega_\nu) \begin{pmatrix} \delta\xi_f^z \\ \delta\xi_c^z \end{pmatrix} \\
& + \begin{pmatrix} \delta\xi_f^+, & \delta\xi_c^+ \end{pmatrix} \boldsymbol{D}_S^{\perp -1}(\boldsymbol{q}, i\omega_\nu) \begin{pmatrix} \delta\xi_f^- \\ \delta\xi_c^- \end{pmatrix} \\
& + \begin{pmatrix} \delta\xi_f^-, & \delta\xi_c^- \end{pmatrix} \boldsymbol{D}_S^{\perp -1}(\boldsymbol{q}, i\omega_\nu) \begin{pmatrix} \delta\xi_f^+ \\ \delta\xi_c^+ \end{pmatrix} \Bigg],
\end{aligned} \tag{19}$$

where the boson propagators split into the following charge and longitudinal spin parts

$$\begin{aligned}
\boldsymbol{D}_C^{-1}(\boldsymbol{q}, i\omega_\nu) &= \begin{pmatrix} J_C[1 - J_C(\overline{\varphi}_2(\boldsymbol{q}, i\omega_\nu) + \overline{\varphi}_m(\boldsymbol{q}, i\omega_\nu))] & -J_C\overline{\varphi}_1(\boldsymbol{q}, i\omega_\nu) \\ -J_C\overline{\varphi}_1(\boldsymbol{q}, i\omega_\nu) & -\overline{\varphi}_{ff}(\boldsymbol{q}, i\omega_\nu) \end{pmatrix}, \\
\boldsymbol{D}_S^{\parallel -1}(\boldsymbol{q}, i\omega_\nu) &= \begin{pmatrix} J_S^2\varphi_{ff}^{\parallel}(\boldsymbol{q}, i\omega_\nu) & J_S[1 + J_S\varphi_{cf}^{\parallel}(\boldsymbol{q}, i\omega_\nu)] \\ J_S[1 + J_S\varphi_{fc}^{\parallel}(\boldsymbol{q}, i\omega_\nu)] & J_S^2\varphi_{cc}^{\parallel}(\boldsymbol{q}, i\omega_\nu) \end{pmatrix}
\end{aligned} \tag{20}$$

and equivalent expression for the transverse spin part $\boldsymbol{D}_S^{\perp -1}(\boldsymbol{q}, i\omega_\nu)$. The expression of the different bubbles are given in the Appendix. The charge boson propagator $\boldsymbol{D}_C(\boldsymbol{q}, i\omega_\nu)$ associated with the Kondo effect is equivalent to that obtained in the $1/N$ expansion theories. The originality of the approach is to simultaneously derive the spin propagator $\boldsymbol{D}_S^{\parallel -1}(\boldsymbol{q}, i\omega_\nu)$ and $\boldsymbol{D}_S^{\perp -1}(\boldsymbol{q}, i\omega_\nu)$ associated with the spin-fluctuation effects. Note that in the magnetically disordered phase, the charge and spin contributions in S_{eff} are totally decoupled.

3.3. Dynamical spin susceptibility

The next step is to consider the dynamical spin susceptibility. For that purpose, we study the linear response M_f to the source-term $-2\boldsymbol{S}_f \cdot \boldsymbol{B}$ (we consider $\boldsymbol{B}$ colinear to the $\boldsymbol{z}$-axis). The effect on the partition function expressed in equation (12) is to change the Hamiltonian $H_J'(\tau)$ to $H_J'^B(\tau)$

$$
\begin{aligned}
&H_J'^B(\tau) = \\
&\sum_{i\sigma\sigma'} \left(c_{i\sigma}^\dagger, f_{i\sigma}^\dagger\right) \begin{pmatrix} -J_S i \boldsymbol{\xi}_{f_i} \cdot \boldsymbol{\tau}_{\sigma\sigma'} & J_C \Phi_i^* \tau_{\sigma\sigma'}^0 \\ J_C \Phi_i \tau_{\sigma\sigma'}^0 & \sum\limits_{\alpha=x,y,z} (-J_S i \xi_{c_i}^\alpha - B\delta_{\alpha z}).\tau_{\sigma\sigma'}^\alpha \end{pmatrix} \begin{pmatrix} c_{i\sigma'} \\ f_{i\sigma'} \end{pmatrix} \\
&+ J_C \sum_i \Phi_i^* \Phi_i + J_S \sum_i \boldsymbol{\xi}_{f_i} . \boldsymbol{\xi}_{c_i} \, . \qquad (21)
\end{aligned}
$$

Introducing the change of variables $\xi_{c_i}^\alpha = \xi_{c_i}^\alpha - iB/J_S$, we connect the f magnetization and the ff dynamical spin susceptibility to the Hubbard–Stratonovich fields $\boldsymbol{\xi}_{f_i}$

$$
\begin{aligned}
M_f^z &= -\frac{1}{\beta} \frac{\partial \ln Z}{\partial B_z} = i \left\langle \xi_{f_i}^z \right\rangle , \\
\chi_{ff}^{\alpha\beta} &= -\frac{1}{\beta} \frac{\partial^2 \ln Z}{\partial B^\alpha \partial B^\beta} = -\left\langle \xi_{f_i}^\alpha \xi_{f_i}^\beta \right\rangle + \left\langle \xi_{f_i}^\alpha \right\rangle \left\langle \xi_{f_i}^\beta \right\rangle . \qquad (22)
\end{aligned}
$$

Using the expression (20) for the boson propagator $\boldsymbol{D}_S^{\parallel -1}(\boldsymbol{q})$, we get for the longitudinal spin susceptibility

$$
\chi_{ff}^{\parallel}(\boldsymbol{q}, i\omega_\nu) = \frac{\varphi_{ff}^{\parallel}(\boldsymbol{q}, i\omega_\nu)}{1 - J_S^2[\varphi_{ff}^{\parallel}(\boldsymbol{q}, i\omega_\nu)\varphi_{cc}^{\parallel}(\boldsymbol{q}, i\omega_\nu) - \varphi_{fc}^{\parallel 2}(\boldsymbol{q}, i\omega_\nu) - \frac{2}{J_S}\varphi_{fc}^{\parallel}(\boldsymbol{q}, i\omega_\nu)]} \qquad (23)
$$

and equivalent expression for the transverse spin susceptibility $\chi_{ff}^{\perp}(\boldsymbol{q}, i\omega_\nu)$. The diagrammatic representation of equation (23) is shown in figure 2. The different bubbles $\varphi_{ff}(\boldsymbol{q}, i\omega_\nu)$, $\varphi_{cc}(\boldsymbol{q}, i\omega_\nu)$ and $\varphi_{fc}(\boldsymbol{q}, i\omega_\nu)$ are evaluated from the expressions of the Green's functions

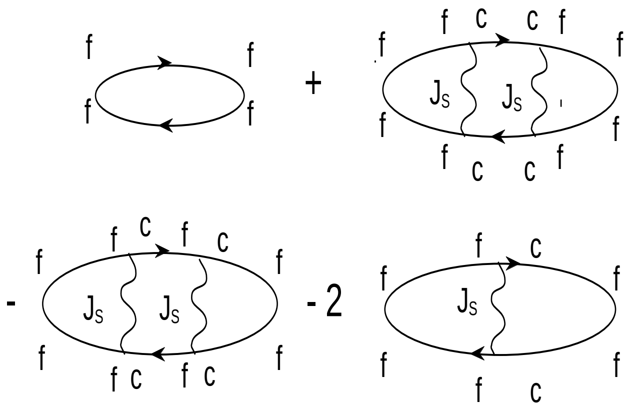

Fig. 2. Diagrammatic representation of equation (23) for the dynamical spin susceptibility $\chi_{ff}(\boldsymbol{q}, \omega)$.

$$
\begin{aligned}
G_{ff}(\boldsymbol{k}, i\omega_n) &= u_k^2 G_{\alpha\alpha}(\boldsymbol{k}, i\omega_n) + v_k^2 G_{\beta\beta}(\boldsymbol{k}, i\omega_n)\,, \\
G_{cc}(\boldsymbol{k}, i\omega_n) &= v_k^2 G_{\alpha\alpha}(\boldsymbol{k}, i\omega_n) + u_k^2 G_{\beta\beta}(\boldsymbol{k}, i\omega_n)\,, \\
G_{cf}(\boldsymbol{k}, i\omega_n) &= G_{fc}(\boldsymbol{k}, i\omega_n) = -u_k v_k [G_{\alpha\alpha}(\boldsymbol{k}, i\omega_n) - G_{\beta\beta}(\boldsymbol{k}, i\omega_n)]\,, \quad (24)
\end{aligned}
$$

where $G_{\alpha\alpha}(\boldsymbol{k}, i\omega_n)$ and $G_{\beta\beta}(\boldsymbol{k}, i\omega_n)$ are the Green's functions associated with the eigenstates $\alpha^\dagger_{k\sigma}|0\rangle$and $\beta^\dagger_{k\sigma}|0\rangle$. In the low-frequency limit, one can easily check that the dynamical spin susceptibility may be written as

$$
\chi_{ff}(\boldsymbol{q}, i\omega_\nu) = \frac{\chi_{\alpha\alpha}(\boldsymbol{q}, i\omega_\nu) + \overline{\chi}_{\alpha\beta}(\boldsymbol{q}, i\omega_\nu)}{1 - J_S^2 \chi_{\alpha\alpha}(\boldsymbol{q}, i\omega_\nu)\overline{\chi}_{\alpha\beta}(\boldsymbol{q}, i\omega_\nu)} \tag{25}
$$

for both the longitudinal and the transverse parts

$$
\begin{aligned}
\chi_{\alpha\alpha}(\boldsymbol{q}, i\omega_\nu) &= \frac{1}{\beta}\sum_k \frac{n_{\mathrm{F}}(E_k^-) - n_{\mathrm{F}}(E_{k+q}^-)}{i\omega_\nu - E_{k+q}^- + E_k^-}\,, \\
\overline{\chi}_{\alpha\beta}(\boldsymbol{q}, i\omega_\nu) &= \frac{1}{\beta}\sum_k (u_k^2 v_{k+q}^2 + v_k^2 u_{k+q}^2)\frac{n_{\mathrm{F}}(E_k^-) - n_{\mathrm{F}}(E_{k+q}^+)}{i\omega_\nu - E_{k+q}^+ + E_k^-}\,.
\end{aligned}
$$

3.4. Physical discussion

From equation (25), one can see that the dynamical spin susceptibility is made of two contributions $\chi_{\mathrm{intra}}(\boldsymbol{q}, i\omega_\nu)$ and $\chi_{\mathrm{inter}}(\boldsymbol{q}, i\omega_\nu)$

$$
\chi_{ff}(\boldsymbol{q}, i\omega_\nu) = \chi_{\mathrm{intra}}(\boldsymbol{q}, i\omega_\nu) + \chi_{\mathrm{inter}}(\boldsymbol{q}, i\omega_\nu) \tag{26}
$$

with

$$\chi_{\rm intra}(\boldsymbol{q},i\omega_\nu)=\frac{\chi_{\alpha\alpha}(\boldsymbol{q},i\omega_\nu)}{1-J_S^2\chi_{\alpha\alpha}(\boldsymbol{q},i\omega_\nu)\overline{\chi}_{\alpha\beta}(\boldsymbol{q},i\omega_\nu)}\,, \qquad (27)$$

$$\chi_{\rm inter}(\boldsymbol{q},i\omega_\nu)=\frac{\overline{\chi}_{\alpha\beta}(\boldsymbol{q},i\omega_\nu)}{1-J_S^2\chi_{\alpha\alpha}(\boldsymbol{q},i\omega_\nu)\overline{\chi}_{\alpha\beta}(\boldsymbol{q},i\omega_\nu)}\,. \qquad (28)$$

$\chi_{\rm intra}(\boldsymbol{q},i\omega_\nu)$and $\chi_{\rm inter}(\boldsymbol{q},i\omega_\nu)$ respectively represent the renormalized particle-hole pair excitations within the lower α band, and from the lower α to the upper β band. The latter expression is reminiscent of the behavior proposed by Bernhoeft and Lonzarich [45] to explain the neutron scattering observed in UPt_3 with the existence of both a "slow" and a "fast" component in $\chi^{"}(\boldsymbol{q},\omega)/\omega$ due to spin-orbit coupling. Also in a phenomenological way, the same type of feature has been suggested in the duality model developed by Kuramoto and Miyake [46]. To our knowledge, the proposed approach provides the first microscopic derivation from the Kondo-lattice model of such a behavior. The bare intraband susceptibility $\chi_{\alpha\alpha}(\boldsymbol{q},\omega)$ is well approximated by a Lorentzian

$$\chi_{\alpha\alpha}^{-1}(\boldsymbol{q},\omega)=\rho_{\alpha\alpha}(\boldsymbol{q})^{-1}\left(1-i\frac{\omega}{\Gamma_0(\boldsymbol{q})}\right)\,, \qquad (29)$$

where $\rho_{\alpha\alpha}=\chi'_{\alpha\alpha}(\boldsymbol{q},0)$ and $\Gamma_0(\boldsymbol{q})$ is the relaxation rate of order $|y_{\rm F}|=T_{\rm K}$. This corresponds to the Lindhard continuum of the intraband particle-hole pair excitations $\chi^{"}_{\alpha\alpha}(q,\omega)\neq 0$ as shown in figure 3. In the same way, one can schematize the low-frequency behavior ($\omega << \omega_0(\boldsymbol{q})$ of the bare interband susceptibility by

$$\overline{\chi}'^{-1}_{\alpha\beta}(\boldsymbol{q},\omega)=\rho_{\alpha\beta}(\boldsymbol{q})^{-1}\left(1-\frac{\omega}{\omega_0(\boldsymbol{q})}\right)\,, \qquad (30)$$

where $\rho_{\alpha\beta}=\overline{\chi}'_{\alpha\beta}(\boldsymbol{q},0)$ and $\omega_0(\boldsymbol{q})$ is a characteristic frequency-scale of the interband transitions. The value of $\omega_0(\boldsymbol{q})$ is strongly structure-dependent. In the simple case of a cubic band structure $\varepsilon_k=-2t(\cos k_x+\cos k_y+\cos k_z)$ (tight-binding scheme including nearest-neighbor hopping), we find a weakly wave-vector dependent frequency around $\boldsymbol{q}=\boldsymbol{Q}$ of order of $\omega_0=2\,|y_{\rm F}|/(\rho_0 J_C)$. The latter result does not stand for more complicated band structures as obtained by de Haas–van Alphen studies combined with band structure calculations in heavy-fermion compounds. In the following, we will leave $\omega_0(\boldsymbol{q})$ as a parameter. Figure 3 shows the continuum of interband particle-hole excitations $\overline{\chi}_{\alpha\beta}" \neq 0$. Due to the presence of the hybridization gap in the density of states, the latter continuum displays a gap equal to $2\sigma_0$, the value

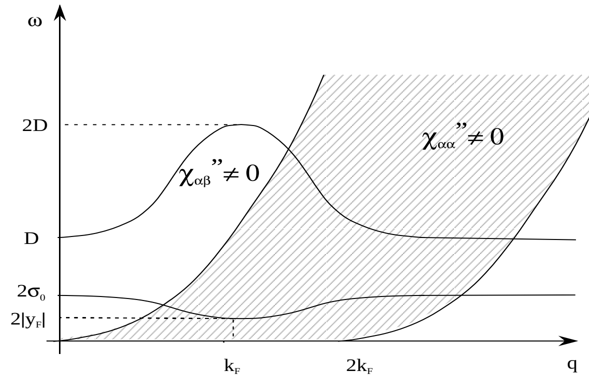

Fig. 3. Continuum of the intraband and interband electron-hole pair excitations $\chi^{''}_{\alpha\alpha}(q,\omega) \neq 0$ and $\chi^{''}_{\alpha\beta}(q,\omega) \neq 0$. Note the presence of a gap in the interband transitions equal to the indirect gap of value $2\,|y_{\rm F}|$ at $q = k_F$, and to the direct gap of value $2\sigma_0$ at $q = 0$.

of the direct gap at $\boldsymbol{q} = \boldsymbol{0}$, and $2\,|y_{\rm F}|$, the value of the indirect gap at $\boldsymbol{q} = \boldsymbol{Q}$ (close to $k_{\rm F}$). More precisely, we have

$$
\begin{aligned}
\overline{\chi}''_{\alpha\beta}(\boldsymbol{0},\omega) &= 4\rho_0 \frac{\sigma_0^2}{\omega\sqrt{\omega^2-4\sigma_0^2}} \qquad \text{at} \quad 2\sigma_0 < \omega < D\,, \\
\overline{\chi}''_{\alpha\beta}(\boldsymbol{Q},\omega) &= 2\rho_0 \frac{1}{1+\omega^2/(2\sigma_0)^2} \quad \text{at} \quad 2\,|y_{\rm F}| < \omega < 2D\,.
\end{aligned} \tag{31}
$$

Far from the antiferromagnetic wave-vector $\boldsymbol{Q} = (\pi,\pi,\pi)$, $\chi_{ff}(\boldsymbol{q},\omega)$ is dominated by the intraband transitions. In the low frequency limit, the frequency dependence of $\chi^{''}_{\rm intra}(\boldsymbol{q},\omega)$ can be approximate to a Lorentzian

$$
\chi^{''}_{ff}(\boldsymbol{q},\omega) \approx \chi^{''}_{\rm intra}(\boldsymbol{q},\omega) = \omega \frac{\chi^{'}_{\rm intra}(\boldsymbol{q})\Gamma_{\rm intra}(\boldsymbol{q})}{\omega^2 + \Gamma_{\rm intra}(\boldsymbol{q})^2} \tag{32}
$$

with

$$
\begin{aligned}
\Gamma_{\rm intra}(\boldsymbol{q}) &= \Gamma_0(\boldsymbol{q})(1-I(\boldsymbol{q}))\,, \\
\chi^{'}_{\rm intra}(\boldsymbol{q}) &= \frac{\rho_{\alpha\alpha}(\boldsymbol{q})}{(1-I(\boldsymbol{q}))}\,.
\end{aligned} \tag{33}
$$

$I(\boldsymbol{q}) = J_S^2\chi'_{\alpha\alpha}(\boldsymbol{q},0)\overline{\chi}'_{\alpha\beta}(\boldsymbol{q},0)$. One has: $\chi'_{\alpha\alpha}(\boldsymbol{0},0) = \rho_{\alpha\alpha}(\boldsymbol{0}) = \rho(E_F)$ and $\chi'_{\alpha\beta}(\boldsymbol{0},0) = \rho_0$. The contribution expressed in equation (32) is consistent with the standard Fermi liquid theory. Note that the product $\Gamma_{\rm intra}(\boldsymbol{q})\chi^{'}_{\rm intra}(\boldsymbol{q})$ $= \rho_{\alpha\alpha}(\boldsymbol{q})\Gamma_0(\boldsymbol{q})$ is independent of I.

Oppositely, at the antiferromagnetic wave-vector $\boldsymbol{Q}$, $\chi_{ff}(\boldsymbol{q},\omega)$ is driven by the interband contribution and we get

$$\chi''_{ff}(\boldsymbol{Q},\omega) \approx \chi''_{\rm inter}(\boldsymbol{Q},\omega) = \omega \frac{I\chi'_{\rm inter}\Gamma_{\rm inter}}{(\omega-\omega_{\rm max})^2+\Gamma^2_{\rm inter}}\,, \tag{34}$$

with

$$\begin{aligned} \omega_{\rm max} &= \omega_0(1-I)\,, \\ \Gamma_{\rm inter} &= \omega_0^2(1-I)/\Gamma_0\,, \\ \chi'_{\rm inter} &= \rho_{\alpha\beta}/(1-I)\,, \end{aligned} \tag{35}$$

where ω_0, $\rho_{\alpha\beta}$, Γ_0 and I are the values of $\omega_0(\boldsymbol{q})$, $\rho_{\alpha\beta}(\boldsymbol{q})$ and $\Gamma_0(\boldsymbol{q})$ and $I(\boldsymbol{q})$ at $\boldsymbol{q}=\boldsymbol{Q}$. The role of the interband transitions have already been pointed out in previous works [47]. However, while the previous studies indicate the presence of an inelastic peak at finite value of the frequency related to the hybridization gap whatever the interaction J is, we emphasize that the renormalization of $\overline{\chi}_{\alpha\beta}(\boldsymbol{Q},\omega)$ into $\chi_{\rm inter}(\boldsymbol{Q},\omega)$ leads to a noteworthy renormalization of the interband gap. Due to the damping introduced by intraband transitions, $\chi''_{\rm inter}(\boldsymbol{Q},\omega)$ takes a finite value at frequency much smaller than the hybridization gap. The relaxation rate $\Gamma_{\rm inter}$ vanishes and the susceptibility $\chi'_{\rm inter}$ diverges at the antiferromagnetic transition with again the product $\Gamma_{\rm inter}\chi'_{\rm inter}$ independent of I. Remarkably, the value $\omega_{\rm max}$ of the maximum of $\chi''_{\rm inter}(\boldsymbol{Q},\omega)/\omega$ is at the same time pushed to zero. This excitation can be analyzed as an excitonic mode which softens at the magnetic transition. Such a behaviour has been effectively observed in $Ce_{1-x}La_xRu_2Si_2$ [18] with a reduction of $\Gamma_{\rm inter}$ and $\omega_{\rm max}$ respectively by a factor 4 and 6 when x goes from 0 to 0.075 so when it gets closer to the magnetic instability occuring at $x=0.08$. It is likely that this mode is called to play a role in the critical phenomena observed near the magnetic transition.

4. The supersymmetric approach

Traditionally, the spin is described either in fermionic or bosonic representation. If the former representation, used for instance in the $1/N$ expansion of the Anderson or the Kondo-lattice models, appears to be well adapted for the description of the Kondo effect, it is also clear that the bosonic representation lends itself better to the study of local magnetism. Quite obviously the physics of heavy-fermions is dominated by the duality between Kondo effect and localized moments. This constitutes the motivation to introduce a new approach to the Kondo lattice model (KLM) which relies on an original representation of the impurity spin 1/2 in which the different degrees of freedom are represented by fermionic as well as bosonic variables. The former are believed to describe the Fermi liquid excitations while the latter account for the residual spin degrees of freedom.

In order to include the Fermi liquid excitations as well as the residual spin degrees of freedom, the proposition is to enlarge the representation of the spin operator as follows

$$S^a = \sum_{\sigma\sigma'} b^\dagger_\sigma \tau^a_{\sigma\sigma'} b_{\sigma'} + f^\dagger_\sigma \tau^a_{\sigma\sigma'} f_{\sigma'} = S^a_b + S^a_f \,, \tag{36}$$

where $b^\dagger_\sigma$ and $f^\dagger_\sigma$ are respectively bosonic and fermionic creation operators and τ^a $(a = (+,-,z))$ are Pauli matrices. Eq. (1) corresponds to a mixed fermionic-bosonic representation between Schwinger bosons and Abrikosov pseudo-fermions. To restrict the dimension of the Hilbert space to two, we introduce the following local constraints

$$n_f + n_b = 1 \,. \tag{37}$$

The constraint restricts the Hilbert space to the two states of the form: $|\uparrow\rangle = (Xb^\dagger_\uparrow + Yf^\dagger_\uparrow)|0\rangle$, $|\downarrow\rangle = (Xb^\dagger_\downarrow + Yf^\dagger_\downarrow)|0\rangle$, where $X^2 + Y^2 = 1$ to guarantee the state normalization to 1 and $|0\rangle$ represents the vacuum of particles: $b_\sigma|0\rangle = f_\sigma|0\rangle = 0$. X and Y are parameters controlling the weight of boson and fermion statistics in the representation: they will be fixed later on by the dynamics. The constraint can be viewed as a charge conservation of the following SU(1|1) fermion-boson rotation symmetry leaving the spin operator invariant

$$\left(f'^\dagger_\sigma, b'^\dagger_\sigma\right) = \left(f^\dagger_\sigma, b^\dagger_\sigma\right) V^\dagger \,, \tag{38}$$

where $V^\dagger$ is an unitary supersymmetric matrix ($VV^\dagger = V^\dagger V = 1$). One can easily check that the representation satisfies the standard rules of SU(2) algebra: $|\uparrow\rangle$ and $|\downarrow\rangle$ are eigenvectors of S^2 and S^z with eigenvalues 3/4 and $\pm 1/2$ respectively, $[S^+, S^-] = 2S^z$ and $[S^z, S^\pm] = \pm S^\pm$ provided that the local constraints expressed in Eq. (2) are satisfied.

In the representation introduced before, the partition function of the three-dimensional KLM can be written as the following path integral

$$Z = \int \mathcal{D}c_{i\sigma}\mathcal{D}f_{i\sigma}\mathcal{D}b_{i\sigma}d\lambda_i \exp\left(-\int_0^\beta d\tau \left(\mathcal{L}(\tau) + \mathcal{H} + \sum_i \lambda_i P_i\right)\right) \tag{39}$$

with

$$\mathcal{L}(\tau) \;=\; \sum_{i\sigma}(c^\dagger_{i\sigma}\partial_\tau c_{i\sigma} + f^\dagger_{i\sigma}\partial_\tau f_{i\sigma} + b^\dagger_{i\sigma}\partial_\tau b_{i\sigma})$$

and

$$\mathcal{H} = \sum_{k\sigma} \varepsilon_k c^\dagger_{k\sigma} c_{k\sigma} + J \sum_i (\boldsymbol{S}_{f_i} + \boldsymbol{S}_{b_i}).\boldsymbol{s}_i - \mu \sum_i n_{c_i} \,.$$

The time-independent Lagrange multiplier λ_i is introduced to enforce the local constraints $P_i = n_{f_i} + n_{b_i} - 1 = 0$. Performing a Hubbard–Stratonovich transformation and neglecting the space and time dependence of the fields in a self-consistent saddle-point approximation, we have

$$\begin{aligned} Z &= \sum_{n=1,2} \int d\eta d\eta^* \mathcal{C}_n\left(\sigma_0, \lambda_0, \eta, \eta*\right) Z_n(\eta, \eta^*) \\ Z_n(\eta,\eta^*) &= \sum_\sigma \int \mathcal{D}c_{i\sigma}\mathcal{D}f_{i\sigma}\mathcal{D}b_{i\sigma} \exp\left(- \int_0^\beta d\tau (\mathcal{L}(\tau) + \mathcal{H}'_{n\sigma}) \right) \end{aligned} \quad (40)$$

with

$$\begin{aligned} \mathcal{H}'_{n\sigma} &= \sum_k (f^\dagger_{k\sigma}, c^\dagger_{k\sigma}, b^\dagger_{k\sigma}) H_0^{n\sigma} \begin{pmatrix} f_{k\sigma} \\ c_{k\sigma} \\ b_{k\sigma} \end{pmatrix}, \\ H_0^{n\sigma} &= \begin{pmatrix} \varepsilon_f & \sigma_0 & 0 \\ \sigma_0 & \varepsilon_k & \eta \\ 0 & \eta^* & \varepsilon_f \end{pmatrix}, \end{aligned}$$

where $\mathcal{C}_n\left(\sigma_0, \lambda_0, \eta, \eta*\right)$ is an integration constant. ε_f is the saddle-point values of the Lagrange multiplier λ_i. Note the presence of a Grassmannian coupling η between $c_{i\sigma}$ and $b_{i\sigma}$, in addition to the usual coupling σ_0 between $c_{i\sigma}$ and $f_{i\sigma}$ responsible for the Kondo effect. In the following, H_0 is indifferently used for any $H_0^{n\sigma}$. H_0 is of the type $\begin{pmatrix} a & \sigma \\ \rho & b \end{pmatrix}$ in which a,b (ρ,σ) are matrices consisting of commuting (anticommuting) variables. Note the supersymmetric structure of the matrix H_0 similar to the supermatrices appearing in the theory of disordered metals [48].

H_0 being Hermitian, the matrix $U^\dagger$ transforming the original basis $\psi^\dagger = \left(f^\dagger, c^\dagger, b^\dagger\right)$ to the basis of eigenvectors $\Phi^\dagger = \left(\alpha^\dagger, \beta^\dagger, \gamma^\dagger\right)$ is unitary ($UU^\dagger = U^\dagger U = 1$). $\Phi^\dagger = \psi^\dagger U^\dagger$ with $U^\dagger$ a supersymmetric matrix. $\alpha^\dagger$ and $\beta^\dagger$ are the fermionic eigenvectors whose eigenvalues, determined from $\det[(a-E) - \sigma(b-E)^{-1}\rho] = 0$, are

$$E_\mp = \frac{(\varepsilon_k + \varepsilon_f) \mp \sqrt{(\varepsilon_k - \varepsilon_f)^2 + 4(\sigma_0^2 + \eta\eta^*)}}{2} \,.$$

$\gamma^\dagger$ is the bosonic eigenvector whose eigenvalue, determined from $\det[(b-E)$ $-\rho(a-E)^{-1}\sigma] = 0$ is $E_\gamma = \varepsilon_f$.

In this scheme, σ_0 and λ_0 are slow variables that we determine by solving saddle-point equations, while η, η^* are fast variables defined by a local approximation. As we will see, the latter approximation incorporates part of the fluctuation effects. Indeed, performing the functional integration of Eq. (40) over the fermion and boson fields [48] yields a superdeterminant (SDet) form written as follows

$$Z(\eta,\eta^*) = S\,\mathrm{Det}\,(\partial_\tau + H_0)\,,$$

where

$$S\,\mathrm{Det}\,(\partial_\tau + H) = \frac{\mathrm{Det}\,(G^{-1} - \sigma D \rho)}{\mathrm{Det}\,(D^{-1})}\,, \qquad (41)$$
$$G^{-1} = \partial_\tau + a \quad \text{and} \quad D^{-1} = \partial_\tau + b\,.$$

Expanding to second order in η, η^* allows us to define the propagator $G_{\eta\eta^*}(\boldsymbol{k}, i\omega_n)$ associated to the Grassmann variable η and hence the closure relation for $x_0^2 = \langle \eta\eta^* \rangle$

$$x_0^2 = \frac{1}{\beta} \sum_{\boldsymbol{k}, i\omega_n} G_{\eta\eta^*}(\boldsymbol{k}, i\omega_n)\ , \qquad (42)$$

with

$$G_{\eta\eta^*}(\boldsymbol{k}, i\omega_n) = \frac{J}{\left[1 - J \Pi^0_{cb}(\boldsymbol{k}, i\omega_n)\right]}$$

and

$$\Pi^0_{cb} = \frac{1}{\beta} \sum_{\boldsymbol{q}, i\omega_n} G_{cc}(\boldsymbol{k}+\boldsymbol{q}, i\omega_n + i\omega_\nu) D(\boldsymbol{q}, i\omega_n)\,.$$

Contrary to [49] which assumes $x_0^2 = 0$ leading to a two-fluid model description, the closure equation Eq. (42) defines a finite x_0^2. This parameter x_0^2 plays a major role in controlling the relative weights of fermion and boson statistics. It is directly connected to the X and Y parameters introduced in the initial representation of the states

$$X^2 = x_0^2/(\sigma_0^2 + x_0^2) \quad \text{and} \quad Y^2 = \sigma_0^2/(\sigma_0^2 + x_0^2)\,.$$

The resolution of the saddle-point equations, keeping the number of particles conserved, leads to

$$\begin{aligned} y_{\mathrm{F}} &= -D \exp\left[-1/(2J\rho_0)\right]\ , \\ 1 &= \frac{2\rho_0(\sigma_0^2 + x_0^2)}{-y_F}\,, \\ \mu &= -\frac{(\sigma_0^2 + x_0^2)}{D}\,. \end{aligned} \qquad (43)$$

Where $y_{\rm F} = \mu - \varepsilon_f$ and $\rho_0 = 1/2D$ is the bare density of states of conduction electrons. From that set of equations, we find : $\varepsilon_f = 0$.

The resulting spectrum of energies is schematized in figure 4. At zero temperature, only the lowest band α is filled with an enhancement of the density of states at the Fermi level (and hence of the mass) unchanged from the standard slave-boson theories $\frac{\rho(E_F)}{\rho_0} = 1 + \frac{(\sigma_0^2 + x_0^2)}{y_F^2} = 1 + \frac{D}{(-y_F)} \gg 1$. This large mass enhancement is related to the flat part of the α band associated with the formation of the Abrikosov–Suhl resonance pinned at the Fermi level. While this feature was already present in the purely fermionic description, it is to be noted that the formation of a dispersionless bosonic band within the hybridization gap is an entirely new result of the theory.

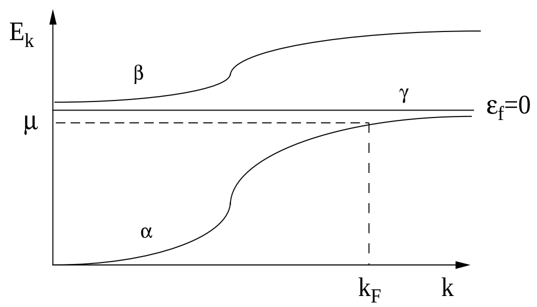

Fig. 4. Sketch of energy versus wave number k for the three bands α, β, γ resulting of the diagonalization of supersymmetric H_0.

The relative weight of boson and fermion statistics in the spin representation is related to x_0^2 : $n_b/n_f = x_0^2/\sigma_0^2$. It is then interesting to follow the J-dependence of x_0^2 as determined by the closure equation (42). The result is shown in Fig. 5. This bell-shaped curve can be interpreted in the light of the exhaustion principle mentioned in the introduction. In the limit of large J, the Kondo temperature-scale $T_{\rm K} = D \exp\left[-1/(2J\rho_0)\right]$ is of order of the bandwidth. One then expects a complete Kondo screening as can be checked by remarking that the weight of c in the α quasiparticle at the Fermi level (noted $v_{k_F}^2$) just equals the added weights of f and b at the Fermi level (respectively noted $u_{k_F}^2$ and ρ_1^2): $v_{k_F}^2/(u_{k_F}^2 + \rho_1^2) = y_F^2/(\sigma_0^2 + x_0^2) = 1$. The Kondo effect being complete in that limit, there is no residual unscreened spin degrees of freedom: it is then natural to derive a zero value of x_0^2 (and hence of n_b). The opposite limit at small J corresponds to the free case of uncoupled impurity spins and conduction electrons. It also leads to: $x_0^2 = 0$. The finite value of x_0^2 between these two limits with a maximum reflects the incomplete Kondo screening effect in the Kondo lattice, the unscreened spin degrees of freedom being described by bosons.

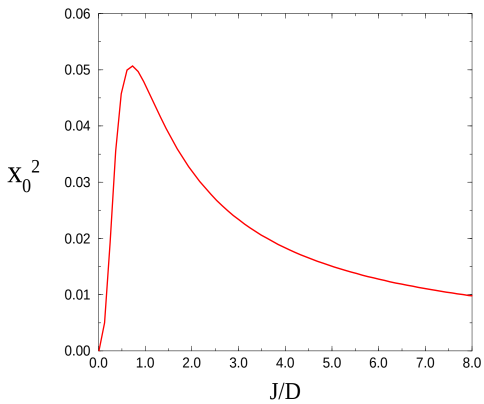

Fig. 5. J/D-dependence of the coupling $x_0^2 = \langle \eta\eta^* \rangle$ fixing the relative weight of fermion and boson statistics. The unit on the vertical-axis is D^2.

Largely discussed in the litterature [20] is the question concerning the Fermi surface sum rule: do the localized spins of the Kondo lattice contribute to the counting of states within the Fermi surface or do they not? Depending on the answer, one expects large or small Fermi surfaces. The supersymmetric theory leads to a firm conclusion in favour of the former. One can check that the number of states within the Fermi surface is just equal to $n_c + n_b + n_f$, *i.e.* $n_c + 1$. The Fermi surface volume includes a contribution of one state per localized spin in addition to that of conduction electrons [20, 50]. The latter conclusion appears sensible if one recalls that the KLM is an effective Hamiltonian derived from the periodic Anderson model (PAM).

Let us now consider the response functions to some external fields namely the dynamical spin susceptibility $\chi^{ab}(\boldsymbol{q},\omega)$ and the frequency-dependent optical conductivity $\sigma^{ab}(\omega)$ $(a,b = x,y,z)$. For that purpose, we introduce the Matsubara correlation functions associated with the operator $\mathcal{O}^a(\boldsymbol{q},\tau)$: $\chi^{ab}(\boldsymbol{q},i\omega_\nu) = \int_0^\beta d\tau \, \exp^{i\omega_\nu\tau} \left\langle T_\tau \mathcal{O}^a(\boldsymbol{q},\tau)\mathcal{O}^b(-\boldsymbol{q},0)\right\rangle$. The operator related to the spin-spin correlation function is the a-component of the spin expressed in the mixed representation introduced in the paper by $S^a(\boldsymbol{q}) = \sum_{k,\sigma,\sigma'} f^\dagger_{k+q,\sigma}\tau^a_{\sigma\sigma'} f_{k,\sigma'} + b^\dagger_{k+q,\sigma}\tau^a_{\sigma\sigma'} b_{k,\sigma'}$. As usual, the dynamical spin susceptibility is then derived from the spin-spin correlation function by the analytical continuation $i\omega_\nu \to \omega + i0^+$. In the same way, the operator related to the current-current correlation function is the a-component of the c-current. In the case of a cubic lattice: $J^a_c(\boldsymbol{q}) = 2\sum_{k,\sigma,\sigma'} \sin k_a c^\dagger_{k+q,\sigma} c_{k,\sigma}$. The frequency-dependent optical conductivity is then obtained from the current-current correlation function by the analytical continuation following: $\sigma^{ab}(\omega) = \left[\chi^{ab}(\boldsymbol{q},\omega+i0^+) - \chi^{ab}(\boldsymbol{q},i0^+)\right] / i\omega$.

By expanding the previous expressions in the basis of the eigenstates $(\alpha^\dagger\beta^\dagger\gamma^\dagger)$ of H_0, we have computed the frequency dependence of $\chi^{ab}(\boldsymbol{Q},\omega)$ at the antiferromagnetic wavevector $\boldsymbol{Q}$ and $\sigma^{ab}(\omega)$ at zero temperature. The two response functions show very different frequency dependence. The frequency-scale at which the dynamical spin susceptibility takes noticeable values is much smaller than for the optical conductivity. This can be understood in the following way. The bosonic γ-band is called to play a role only when spin is concerned namely for the dynamical spin susceptibility. That feature comes from the fact that the spin is related to both fermionic and bosonic operators while the c-current is simply expressed within fermionic operators. Therefore, one can show that the dynamical spin susceptibility involves transitions between all three bands α, β and γ. The main contribution for $\chi^{ab}(\boldsymbol{Q},\omega)$ is due to the particle-hole pair excitations from the fermionic α to the bosonic γ band. Oppositely, the optical conductivity is associated with transitions between fermionic bands only. As can be seen in figure 6, a gap appears in the frequency dependence of $\sigma(\omega)$ equal to

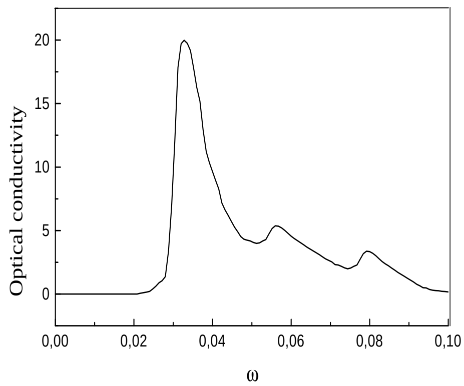

Fig. 6. Frequency-dependence of the optical conductivity $\sigma(\omega)$ at $T = 0$ for $D = 0.8$ and $T_{\rm K} = 0.001$.

the direct gap between the α and β bands. The latter result agrees with the predictions of the dynamical mean-field theory in the limit of infinite dimensions [51]. The whole discussion clarifies the physical content of the novel bosonic mode brought by the supersymmetric approach. That mode is related to the spin excitations. It introduces new features in the dynamical spin susceptibility by comparison to the standard slave-boson theories while it does not affect the optical conductivity.

5. Conclusion

Important progress has been made the last years in the understanding of the Kondo-lattice model with the development of new functional integral approaches. They have enlightened as to the nature of the ground state and the existence of collective modes. They open up new prospects for the description of the critical phenomena associated to the quantum phase transition in heavy-fermion systems. A complete study of the quantum phase transition will probably requires the use of the Group Renormalization techniques for which the functional integral approaches presented here might constitute the framework.

We would like to thank N.R. Bernhoeft, P. Coleman, P.A. Lee, G.G. Lonzarich, K. Miyake, M.J. Rozenberg, J. Spalek for many interesting and helpful discussions.

Appendix A

The expressions of the different bubbles appearing in the expression of the boson propagators (*cf.* Eq. (20) are given here (with i=1, 2, m or ff)

$$
\begin{aligned}
\overline{\varphi}_i(\boldsymbol{q}, i\omega_\nu) &= \varphi_i(\boldsymbol{q}, i\omega_\nu) + \varphi_i(-\boldsymbol{q}, -i\omega_\nu)\,, \\
\varphi_1(\boldsymbol{q}, i\omega_\nu) &= -\frac{1}{\beta}\sum_{k\sigma, i\omega_n} G^\sigma_{cf0}(\boldsymbol{k}+q, i\omega_n + i\omega_\nu) G^\sigma_{ff0}(\boldsymbol{k}, i\omega_n)\,, \\
\varphi_2(\boldsymbol{q}, i\omega_\nu) &= -\frac{1}{\beta}\sum_{k\sigma, i\omega_n} G^\sigma_{cc0}(\boldsymbol{k}+\boldsymbol{q}, i\omega_n + i\omega_\nu) G^\sigma_{ff0}(\boldsymbol{k}, i\omega_n)\,, \\
\varphi_m(\boldsymbol{q}, i\omega_\nu) &= -\frac{1}{\beta}\sum_{k\sigma, i\omega_n} G^\sigma_{cf0}(\boldsymbol{k}+\boldsymbol{q}, i\omega_n + i\omega_\nu) G^\sigma_{cf0}(\boldsymbol{k}, i\omega_n)\,,
\end{aligned}
$$

$$
\begin{aligned}
\varphi^{\|}_{ff}(\boldsymbol{q}, i\omega_\nu) &= -\frac{1}{\beta}\sum_{k\sigma, i\omega_n} G^\sigma_{ff0}(\boldsymbol{k}+\boldsymbol{q}, i\omega_n + i\omega_\nu) G^\sigma_{ff0}(\boldsymbol{k}, i\omega_n)\,, \\
\varphi^{\|}_{cc}(\boldsymbol{q}, i\omega_\nu) &= -\frac{1}{\beta}\sum_{k\sigma, i\omega_n} G^\sigma_{cc0}(\boldsymbol{k}+\boldsymbol{q}, i\omega_n + i\omega_\nu) G^\sigma_{cc0}(\boldsymbol{k}, i\omega_n)\,, \\
\varphi^{\|}_{fc}(\boldsymbol{q}, i\omega_\nu) &= -\frac{1}{\beta}\sum_{k\sigma, i\omega_n} G^\sigma_{fc0}(\boldsymbol{k}+\boldsymbol{q}, i\omega_n + i\omega_\nu) G^\sigma_{fc0}(\boldsymbol{k}, i\omega_n)\,, \qquad (44)
\end{aligned}
$$

$$\varphi^{\perp}_{ff}(\boldsymbol{q}, i\omega_\nu) = -\frac{1}{\beta} \sum_{k\sigma, i\omega_n} G^{\uparrow}_{ff0}(\boldsymbol{k}+\boldsymbol{q}, i\omega_n + i\omega_\nu) G^{\downarrow}_{ff0}(\boldsymbol{k}, i\omega_n)\,,$$
$$\varphi^{\perp}_{cc}(\boldsymbol{q}, i\omega_\nu) = -\frac{1}{\beta} \sum_{k\sigma, i\omega_n} G^{\uparrow}_{cc0}(\boldsymbol{k}+\boldsymbol{q}, i\omega_n + i\omega_\nu) G^{\downarrow}_{cc0}(\boldsymbol{k}, i\omega_n)\,,$$
$$\varphi^{\perp}_{fc}(\boldsymbol{q}, i\omega_\nu) = -\frac{1}{\beta} \sum_{k\sigma, i\omega_n} G^{\uparrow}_{fc0}(\boldsymbol{k}+\boldsymbol{q}, i\omega_n + i\omega_\nu) G^{\downarrow}_{fc0}(\boldsymbol{k}, i\omega_n)\,, \quad (45)$$

where $G^{\sigma}_{cc0}(\boldsymbol{k}, i\omega_n)$, $G^{\sigma}_{ff0}(\boldsymbol{k}, i\omega_n)$ and $G^{\sigma}_{fc0}(\boldsymbol{k}, i\omega_n)$ are the Green's functions at the saddle-point level obtained by inversing the matrix $G^{\sigma}_0(\boldsymbol{k}, \tau)$ defined in equation (13).

REFERENCES

[1] For a review see P.A. Lee, T.M. Rice, J.W. Serene, L.J. Sham, J.W. Wilkins, *Comments Condens. Matter Phys.* **12**, 99 (1986); D.M. Newns, N. Read, *Adv. Phys.* **36**, 799 (1987); P. Fulde, J. Keller, G. Zwicknagl, in *Solid State Physics*, vol. 41, edited by H. Ehrenreich and D. Turnbull, Academic, New York 1988; N. Grewe, F. Steglich, in *Handbook on the Physics and Chemistry of the Rare Earths*, vol.14, North Holland, Amsterdam 1990.

[2] S.R. Julian, P.A.A. Teunissen, S.A.J. Wiegers, *Phys. Rev.* **B46**, 9821 (1992); S.R. Julian, F.S. Tautz, G.J. McMullan, G.G. Lonzarich, *Physica B* **199 & 200**, 63 (1994).

[3] S. Doniach, *Physica B* **91**, 231 (1977).

[4] H. von Löhneysen, T. Pietrus, G. Portisch, H.G. Schlager, A.C. Schröder, M. Sieck, T. Trappmann, *Phys. Rev. Lett.* **72**, 3262 (1994); H. von Löhneysen, *J. Phys. Condens. Matter* **8**, 9689 (1996).

[5] S.R. Julian, C. Pfleiderer, F.M. Grosche, N.D. Mathur, G.J. McMullan, A.J. Diver, I.R. Walker, G.G. Lonzarich, *J. Phys. Condens. Matter* **8**, 9675 (1996).

[6] F. Steglich, B. Buschinger, P. Gegenwart, M. Lohmann, R. Helfrich; C. Langhammer, P. Hellmann, L. Donnevert, S. Thomas, A. Link, C. Geiber, M. Lang, G. Sparn, W. Assmus, *J. Phys. Condens. Matter* **8**, 9909 (1996) .

[7] S. Kambe, S. Raymond, L.P. Regnault, J. Flouquet, P. Lejay, P. Haen, *J. Phys. Soc. Jpn.* **65**, 3294 (1996).

[8] D.L. Cox, *Phys. Rev. Lett.* **59**, 1240 (1987); D.L. Cox, M. Jarrell, *J. Phys. Condens. Matter* **8**, 9825 (1996).

[9] V. Dobrosavljevic, T.R. Kirkpatrick, G. Kotliar, *Phys. Rev. Lett.*, **69**, 1113 (1992); E. Miranda, V. Dobrosavljevic, G. Kotliar *J. Phys. Condens. Matter* **8**, 9871 (1996).

[10] J.A. Hertz, *Phys.Rev.* **B14**, 1165 (1976).
[11] A.J. Millis, *Phys. Rev.* **B48**, 7183 (1993).
[12] T. Moriya, T. Takimoto, *J. Phys. Soc. Jpn.* **64**, 960 (1995).
[13] M.A. Continentino, *Phys. Rev.* **B47**, 11581 (1993).
[14] A. Rosch, A. Schröder, O. Stockert, H. v.Löhneysen, *Phys. Rev. Lett.* **79**, 159 (1997).
[15] C. Pépin, M. Lavagna, to be published in *Phys. Rev.* **B**.
[16] L.P. Regnault, W.A.C. Erkelens, J. Rossat-Mignod, P. Lejay, J. Flouquet, *Phys. Rev.* **B38**, 4481 (1988); S. Raymond, L.P. Regnault, S. Kambe, J.M. Mignod, P. Lejay, J. Flouquet, *J. Low Temp. Phys.* **109**, 205 (1997).
[17] G. Aeppli, C. Broholm in *Handbook on the Physics and Chemistry of Rare Earths*, vol.19, 123, ed. by Gschneidner *et al.*, Elsevier, 1994 and references therein .
[18] S. Raymond, L.P. Regnault, S. Kambe, J.M. Mignod, P. Lejay, J. Flouquet, *J. Low Temp. Phys.* **109**, 205 (1997).
[19] P.W. Anderson, *Phys. Rev.* **B124**, 41 (1961).
[20] H. Tsunetsugu, M. Sigrist, K. Ueda, *Rev. Mod. Phys.* **69**, 809 (1997) and references therein.
[21] P. Nozières, *Ann. Phys. (Paris)* **10**, 19 (1985).
[22] P. Coleman, *Phys. Rev.* **B29**, 3035 (1984).
[23] N. Read, D.N. Newns, *J. Phys.* **C16**, 3273 (1983).
[24] A.J. Millis, P.A. Lee, *Phys. Rev.* **B35**, 3394 (1987).
[25] A. Auerbach, K. Levin, *Phys. Rev. Lett.* **57**, 877 (1986).
[26] M. Lavagna, A.J. Millis, P.A. Lee, *Phys. Rev. Lett.* **58**, 266 (1987).
[27] N. Read, D.M. Newns, S. Doniach, *Phys. Rev.* **B30**, 3841 (1984).
[28] J. Kroha, P. Wolfle, T.A. Costi, *Phys. Rev. Lett.* **79**, 261 (1997).
[29] A. Houghton, N. Read, H. Won, *Phys. Rev.* **B37**, 3782 (1988).
[30] G. Kotliar, A.E. Ruckenstein, *Phys. Rev. Lett.* **57**, 1362 (1986).
[31] T.M. Rice, K. Ueda, *Phys. Rev. Lett.* **55**, 995 (1985).
[32] T. Li, P. Wolfle, P.J. Hirschfeld, *Phys. Rev.* **B40**, 6817 (1989).
[33] M. Lavagna, *Phys. Rev.* **B41**, 142 (1990).
[34] M.F. Yang, S.J. Sun, T.M. Hong, *Phys. Rev.* **B48**, 16123 (1993).
[35] Z. Gulacsi, R. Strack, D. Vollhardt, *Phys. Rev.* **B47**, 8594 (1993).
[36] S.J. Sun, M.F. Yang, T.M. Hong, *Phys. Rev.* **B48**, 16127 (1993).
[37] M. Jarrell, H. Akhlaghpour, T. Pruschke, *Phys. Rev. Lett.* **70**, 1670 (1993).
[38] M.J. Rozenberg, *Phys. Rev.* **B52**, 7369 (1995).
[39] R. Doradziński, J. Spalek, *Phys. Rev.* **B56**, R14239 (1997); R. Doradziński, J. Spalek, *Phys. Rev.* **B58**, 1 (1998).
[40] B. Moller, P. Wolfle, *Phys. Rev.* **B48**, 10320 (1993).
[41] C. Lacroix, M. Cyrot, *Phys. Rev.* **B20**, 1969 (1979).

[42] P. Coleman, N. Andrei, *J. Phys., Condens. Matter* **1**, 4057 (1989).

[43] J.R. Iglesias, C. Lacroix, B. Coqblin, *Phys. Rev.* **B56**, 11820 (1997).

[44] C. Pépin, M. Lavagna, *Z. Phys.* **B103**, 259 (1997); C. Pépin, M. Lavagna, Cond-mat9709256.

[45] N.R. Bernhoeft, G.G. Lonzarich, *J. Phys. Condens. Matter* **7**, 7325 (1995).

[46] Y. Kuramoto, K. Miyake, *J. Phys. Soc. Jpn.* **59**, 2831 (1990).

[47] A. Auerbach, J.H. Kim, K. Levin, M.R. Norman, *Phys. Rev. Lett.* **60**, 623 (1988).

[48] K.B. Efetov, *Adv. Phys.* **32**, 53 (1983).

[49] J. Gan, P. Coleman, N. Andrei, *Phys. Rev. Lett.* **68**, 3476 (1992).

[50] R.M. Martin, *Phys. Rev. Lett.* **48**, 362 (1982).

[51] M.J. Rozenberg, G. Kotliar, H. Kajueter, *Phys. Rev.* **B54**, 8452 (1996).